

The Impact of Uni-axial Strain and Dynamic Body Biases on Low Frequency Noise in Nanoscale pMOSFETs

Kuo-Liang Yeh, Chih-You Ku, Wei-Lun Hong, and Jyh-Chyurn Guo
Institute of Electronics Engineering, National Chiao Tung University, Hsinchu, Taiwan
Tel: +886-3-5131368, Fax: +886-3-5724361, E-mail: jcguo@mail.nctu.edu.tw

Abstract

The impact of local strain on low frequency noise (LFN) is investigated under dynamic body biases. For 60 nm pMOS, the uni-axial compressive strain from e-SiGe can contribute 75% effective mobility (μ_{eff}) enhancement and near 80% boost in current (I_{DS}) as well as transconductance (G_m). However, the strained pMOS suffer more than 80% higher LFN ($S_{\text{ID}}/I_{\text{D}}^2$) and the increase of Hooge parameter (α_{H}) in mobility fluctuation model is identified as the key factor. Forward body biases (FBB) can reduce LFN attributed to reduced normal field (E_{eff}), but reverse body bias (RBB) enhance LFN due to enhanced E_{eff} . Both the benefit from FBB and loss from RBB become insignificant in strained pMOSFETs at a nanoscale dimension.

I. Introduction

Strain engineering has evolved as an indispensable technology for mobility enhancement and current boost at 65 nm node and beyond [1]. However, the potential impact on noise, particularly the low frequency noise (LFN), brings a critical challenge. Maeda *et al.* reported flicker noise increase in pMOS under both compressive and tensile stress, namely bi-directional noise degradation[2]. Stress induced traps and dipoles were assumed responsible for flicker noise degradation. However, Ueno *et al.* claimed improved 1/f noise in strained pMOS with e-SiGe [3]. In this paper, a novel and interesting result of uni-axial compressive strain effect on LFN in pMOS under dynamic body biases is presented. Mobility fluctuation model can be used to explain the strain and dynamic body biases effect in nanoscale pMOS.

II. Experimental

As shown in Fig.1, strained pMOS with e-SiGe in S/D for uni-axial compressive strain were fabricated in 65 nm process and the standard pMOS free from strain engineering act as the control devices. The power spectral density (PSD) of drain current noise, namely S_{ID} was measured by LFN measurement system, consisting of Agilent dynamic signal analyzer (DSA 35670) and low noise amplifier (LNA SR570). The LFN measurement generally covers a wide frequency range of 10~100K Hz.

II. Results and Discussion

Fig.2 indicates that the uni-axial compressive strain can realize around 78% boost in I_{DS} and G_m for 60 nm pMOS. Interestingly, the μ_{eff} extracted from linear I-V shown in Fig. 3 exhibits a significant dependence on gate length (L_g). For shorter L_g , strained pMOS gains higher μ_{eff} but control pMOS suffers a dramatic degradation in μ_{eff} . As a result, the μ_{eff} enhancement due to this local strain can attain 75% for 60 nm devices, which contributes near 80% increase in I_{DS} and G_m as demonstrated. Furthermore, this μ_{eff} enhancement leads to 65% higher I_{DS} in saturation region, shown in Fig.4. Fig.5(a) presents V_T vs. L_g with a dramatic difference due to this uni-axial strain. The control pMOS show an apparent RSCE but the strained pMOS reveal a V_T roll off for L_g scaling to 60 nm. Fig.5(b) exhibits V_T shift (ΔV_T) under forward and reverse body biases (FBB/RBB $V_{\text{BS}}=-0.6/0.6\text{V}$). Note that strained pMOS have a smaller ΔV_T under both FBB and RBB, particularly for 60 nm device due to a

V_T roll off. This feature will influence dynamic body bias effect on μ_{eff} and LFN.

Fig. 6 indicates a remarkably faster increase of $S_{\text{ID}}/I_{\text{D}}^2$ with L_g scaling for strained pMOS and more than 80% higher $S_{\text{ID}}/I_{\text{D}}^2$ in 60 nm devices. These results cannot be explained by number fluctuation model[4]. Referring to Fig.5(a), the dramatic RSCE in control pMOS suggests a highly non-uniform channel doping profile and potentially worse LFN based on number fluctuation model [4]. However, the experimental for pMOS exhibits an opposite trend. Fig.7 shows an analysis of LFN in terms of $S_{\text{ID}}/I_{\text{D}}^2$ vs. I_{DS} under various V_{GT} and V_{BS} . The $S_{\text{ID}}/I_{\text{D}}^2$ follows a function proportional to $1/I_{\text{DS}}$, which can be described by Hooge's mobility fluctuation model [5] given in (1). Note that the mobility fluctuation model in (1) is useful to predict the dependence on device parameters (W , L , C_{ox} , μ_{eff} , α_{H}), I_{DS} , V_{GT} , and to explore the origins responsible for the worse LFN in strained pMOS. The increase of μ_{eff} and Hooge parameter α_{H} will lead to higher $S_{\text{ID}}/I_{\text{D}}^2$ under a specified I_{DS} . It explains why the strained pMOS with short L_g indeed gain higher μ_{eff} but suffer worse LFN. Fig.8 exhibits a remarkable increase of α_{H} with L_g scaling in strained devices and suggests that local strain may increase α_{H} and make LFN worse. The enlarged difference in α_{H} with L_g scaling is the major factor responsible for the substantial difference in $S_{\text{ID}}/I_{\text{D}}^2$. An accelerated phonon scattering in strained lattice is considered the potential mechanism responsible for increase of α_{H} in strained pMOS [6]. Fig. 9 displays dynamic body biases effect on LFN in terms of $\Delta S_{\text{ID}}(V_{\text{BS}})/S_{\text{ID}}(V_{\text{BS}}=0)$, $\Delta S_{\text{ID}}(V_{\text{BS}})=S_{\text{ID}}(V_{\text{BS}})-S_{\text{ID}}(V_{\text{BS}}=0)$ under FBB ($V_{\text{BS}}=-0.6\text{V}$) and RBB ($V_{\text{BS}}=0.6\text{V}$). For both strained and control pMOS, FBB can reduce S_{ID} ($\Delta S_{\text{ID}}(V_{\text{BS}})<0$) whereas RBB makes LFN worse ($\Delta S_{\text{ID}}(V_{\text{BS}})>0$). However, the dynamic body biases effect on LFN is degraded in strained pMOS with a smaller amount of $\Delta S_{\text{ID}}(V_{\text{BS}})/S_{\text{ID}}(V_{\text{BS}}=0)$. The critical dependence of α_{H} on μ_{eff} shown in Fig. 10 can facilitate an understanding of the mechanism responsible for dynamic body biases effect on LFN. FBB can help increase μ_{eff} under a specified V_{GT} due to smaller normal field (E_{eff}) resulted from reduced body depletion charge. The increase of μ_{eff} in this way can achieve lower α_{H} and then realize lower LFN. On the other hand, the μ_{eff} enhancement from the uni-axial strain is accompanied with larger α_{H} and leads to the penalty of worse LFN.

$$\frac{S_{\text{ID}}}{I_{\text{DS}}^2} = \frac{1}{f} \frac{qV_{\text{DS}}}{I_{\text{DS}}} \frac{\alpha_{\text{H}}\mu_{\text{eff}}}{L^2} \quad (1)$$

Acknowledgement

This work is supported in part by *NSC 97-2221-E009-175*. Besides, the authors acknowledge the support from ND Lab. for noise measurement and UMC R&D for device fabrication

References

- [1] P. Bai, *et al.*, *IEDM Tech. Digest*, Dec. 2004, p. 657
- [2] S. Maeda, *et al.*, *VLSI Tech. Symp. Proc.*, June 2004, p.102
- [3] T. Ueno, *et al.*, *VLSI Tech. Symp. Proc.*, June 2006, p.104
- [4] J.-W. Wu, *et al.*, *IEEE TED-51*, no.8, p.1262, 2004
- [5] F. N. Hooge, *et al.*, *Phys. Lett. A*, vol. 66, p. 315, 1978.
- [6] R. P. Jindal, *et al.*, *J. Appl. Phys.* vol.52, no. 4, p. 2884 1981

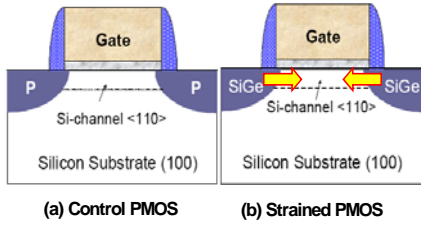


Fig. 1 (a) control pMOS without strain (b) strained pMOS with e-SiGe in S/D for compressive strain

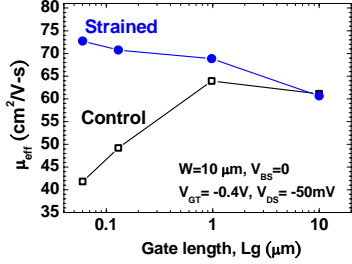


Fig. 3 μ_{eff} vs. L_g (10~0.06 μm) for strained and control pMOS

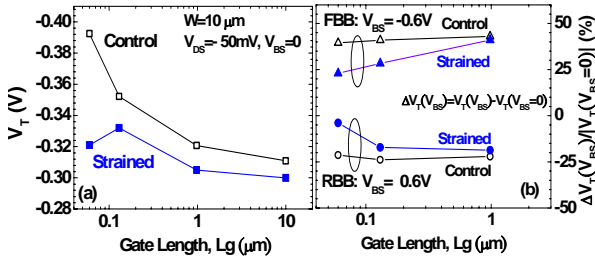


Fig. 5 (a) Linear V_T ($V_{DS}=-50\text{mV}$, $V_{BS}=0$) vs. L_g (1 ~0.06 μm) (b) $\Delta V_T(V_{BS})/V_T(V_{BS}=0)$, $\Delta V_T(V_{BS})-V_T(V_{BS}=0)$ under FBB ($V_{BS}=-0.6\text{V}$) and RBB ($V_{BS}=0.6\text{V}$) for strained and

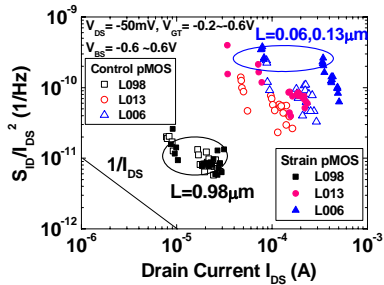


Fig. 7 The S_{ID}/I_{DS}^2 vs. I_{DS} under varying V_{GT} ($V_{GT}=-0.2\sim-0.6\text{V}$) and $V_{BS}=-0.6, 0, 0.6\text{V}$ for strained and control pMOS ($L_g=0.98\sim0.06\mu\text{m}$).

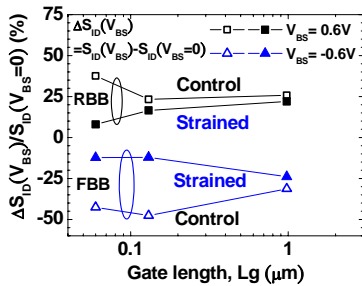


Fig. 9 $\Delta S_{ID}(V_{BS})/S_{ID}(V_{BS}=0)$ under FBB ($V_{BS}=-0.6\text{V}$) and RBB ($V_{BS}=0.6\text{V}$) for strained & control pMOS (0.98 ~0.06 μm)

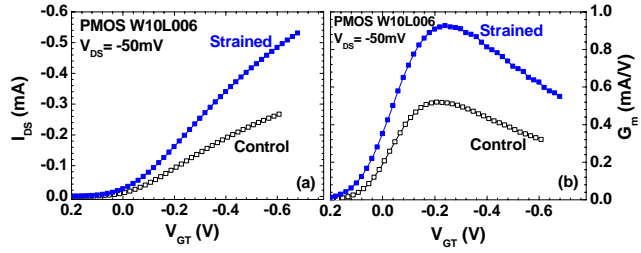


Fig. 2 (a) I_{DS} vs. V_{GT} (b) G_m vs. V_{GT} measured in linear region at $V_{DS}=-50\text{mV}$ for control and strained pMOSFETs with $L_g=60\text{nm}$

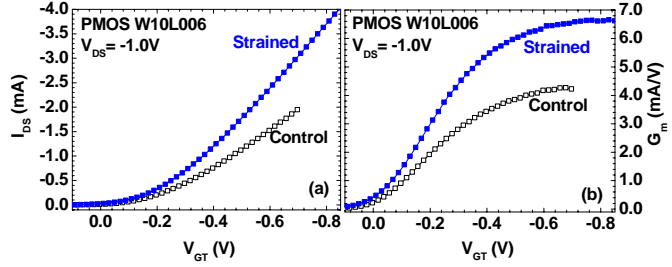


Fig. 4 (a) I_{DS} vs. V_{GT} (b) G_m vs. V_{GT} measured in saturation region at $V_{DS}=-1\text{V}$ for control and strained pMOSFETs with $L_g=60\text{nm}$

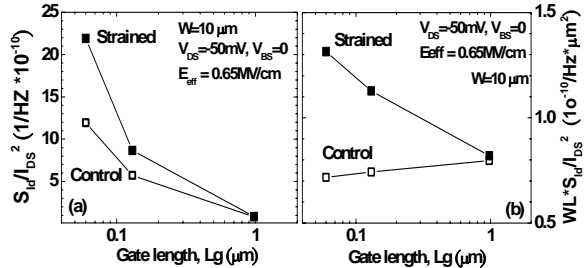


Fig. 6 The S_{ID}/I_{DS}^2 measured under E_{eff} of 0.65MV/cm for strained and control pMOS with various L_g (0.98 ~0.06 μm) (a) S_{ID}/I_{DS}^2 (b) $S_{ID}/I_{DS}^2 \times WL_g$

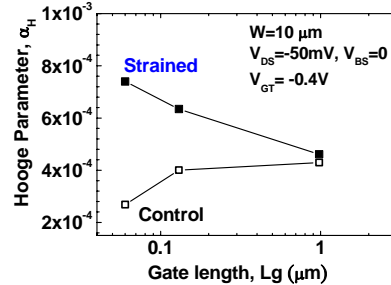


Fig. 8 Hooge parameter α_H vs. L_g (0.98 ~0.06 μm) strained and control pMOS extracted from S_{ID}/I_{DS}^2 at $V_{GT}=-0.4\text{V}$, $V_{BS}=0$.

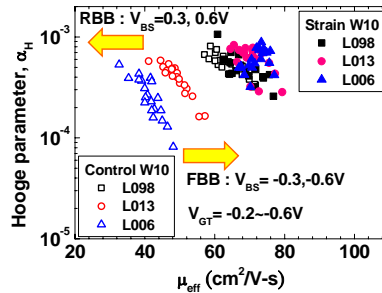


Fig. 10 Hooge parameter α_H vs. μ_{eff} under FBB ($V_{BS}=-0.3, -0.6\text{V}$) and RBB ($V_{BS}=0.3, 0.6\text{V}$). FBB can increase μ_{eff} and reduce α_H